

Performance indicators for coupling desalination plants with wave energy

B. Del Río-Gamero^{a,*}, Tyrone Lis Alecio^b, J. Schallenberg-Rodríguez^a

^a Industrial and Civil Engineering School, Universidad de Las Palmas de Gran Canaria, Las Palmas de Gran Canaria, Spain

^b Oceanic Platform of the Canary Islands (PLOCAN), Telde, Spain

HIGHLIGHTS

- Desalination plants energy demand are supplied by wave energy farms.
- Performance indicators were established for analysing wave energy converters.
- Different wave technologies and desalination plants have been used.
- A parametrization for this indicators is done in order to extrapolate to any plant.

ARTICLE INFO

Keywords:

Wave energy
Desalination
Performance indicators
Wave energy converters
Wave resource

ABSTRACT

This research work addresses the challenge of supplying desalination plants with electricity from waves. The vast majority of desalination plants are located in coastal areas, making wave energy a potential and viable cornerstone for the desalination sector. A series of performance indicators, such as freshwater production per sea covered area, are established and used in this study to evaluate different wave energy converters (WECs). Analyses of the performance of wave farms are undertaken. Some of the indicators are parameterized with the intention of extrapolating the results to other desalination plants, using the specific energy consumption of the desalination plant or the sea surface area covered by WECs. The study is developed for mid-range wave climates, comparing two zones with different sea conditions in order to establish correlations. The Canary Islands (Spain), where more than 600,000 m³ of desalinated water are produced each day, is the selected scenario. Results show that no correlation could be established between the wave resource and WEC output and confirm the need to simultaneously analyze the wave resource and the behavior of each technology in the selected marine area. It is also found that higher wave energy potential does not necessarily lead to higher energy production. Results also show that WECs can supply an important percentage of the desalination plant electricity demand and wave farm configurations have more similarities than single devices in terms of technologies.

1. Introduction

In the transition towards more sustainable energy production, marine renewable energies are a key factor in coastal regions [1–4]. This situation is accentuated in regions whose waters isolate the territory (limiting electrical grid interconnections), such as islands [5,6]. Offshore wind power technologies are currently playing a major role in this transition [7–10], but wave technologies have an even greater potential in areas where the wave resource is more concentrated and continuous compared to wind energy [11].

The location of marine technologies close to the coast makes it essential to have nearby facilities whose energy demand can be met by

such technologies. In this regard, many of the more than 2200 inhabited islands in the European Union [12] have undergone a transformation in recent decades in how they obtain their water resources [13]. This transformation includes the implementation of desalination plants (mainly reverse osmosis technology) whose electricity consumption often figures high in the island electricity mix [14–16]. To date, many reviews on the application of renewable energies to desalination processes have been carried out [17–21]. This subject is so relevant that the Desalination Journal published a special issue in 2018 that included 25 peer reviews papers [22]. In most reviews, wave energy was mentioned as a possibility to supply desalination plants, but it is not until 2021 when a review work placed this resource as a serious alternative to

* Corresponding author.

E-mail address: beatriz.delrio@ulpgc.es (B. Del Río-Gamero).

<https://doi.org/10.1016/j.desal.2021.115479>

Received 25 August 2021; Received in revised form 23 November 2021; Accepted 26 November 2021

Available online 9 December 2021

0011-9164/© 2021 The Authors.

Published by Elsevier B.V. This is an open access article under the CC BY-NC-ND license

(<http://creativecommons.org/licenses/by-nc-nd/4.0/>).

supply desalination plants [23].

This work focuses on the Canary Islands (Spain), a worldwide benchmark location for desalination plants [24]. The objective is to analyze the possible implementation of wave power to meet the electricity demand of desalination plants. To do so, performance indicators were developed that consider the adaptability of wave energy converters (WECs) to desalination plants depending on the wave resource, the required sea surface area, the percentage of desalination plant energy demand coverage, and the energy density, among others.

In terms of the wave resource, areas with the highest mean wave power density were initially considered the most suitable for WEC implementation, but the temporal variability of the wave resource was not taken into consideration [25]. However, assessments based on shorter periods (monthly or seasonal) provided valuable insights into this temporal variation [26,27]. Recent studies have shown that inter-annual fluctuations can be significant and must be taken into consideration when selecting the area for WEC installation [28,29]. Both short- and long-term variability of the resource play an important role in the financial returns of wave energy farms. It should also be noted that long-term data series are vital for the accuracy of an analysis. When variations in wave resources have been analyzed, most cases have adopted the recommendation of the World Meteorological Organization and used 30–40 years of data to obtain a reliable estimation of the wave climate [30]. From a general perspective, the works carried out by researchers in the wave sector can be classified into two strands: one analyzing the wave resource and its long-term inter- and intra-annual variabilities, and the other focusing on WECs and how they can be affected by the wave resource over short periods of time. This work combines both analysis and demonstrate that this combination is able to achieve results that are more accurate. For this reason, in this study, the wave resource is analyzed in series exceeding 20 years and an intra-annual analysis at monthly level is also carried out with the aim of observing the adaptability of WECs to desalination plants in a detailed way. The longer the period of historical data, the better the understanding of the resource, and more precisely the future resource can be predicted [27]. In such situations, while the configuration of WECs or WEC farms using scatter diagrams is based on past resource data, it can potentially be optimized in view of potential changes in the wave energy resource [31]. The present study does not suffer the problem of the non-availability of an extensive database [32], a problem that is exacerbated if two locations are to be compared (as an example the work of Kamranzad et al., in 2017 which analyzes 25 years of data [33]).

As regards WECs, while it is true that this technology is not yet mature, a wide variety of devices are currently being developed with the aim of harnessing the energy of the waves to produce electricity [34]. In this regard, it has been confirmed that there is no single WEC that presents the best performance globally [35]. As an example, in the aforementioned study [35], the energy production of the WaveStar WEC was found to be comparatively lower than that of the Wave Dragon and Oyster WECs, whereas another study found the WaveStar to be the most versatile of 6 WECs on the Greek coasts [36].

The above research studies only considered a single WEC and did not validate the effect of wave resource variations for wave farms. For this, it is necessary to take into account wake effects in array configurations. In one of the first studies to show these effects on different farms situated off the Calabrian coast, it was confirmed that such an analysis was important to find the optimal WEC and preserve the wave energy production level [37]. The vast majority of the desalination plants installed in the Canary Islands have an installed power that needs to be covered by more than one WEC. This work therefore focuses on wave farms located in the Atlantic Ocean (latitude: 28° 17' 29.6340" N and longitude: 16° 37' 44.8644" W coordinates), where the local characteristics of wave height and period differ greatly from the Aegean Sea or the Calabrian coast.

In the literature search that was conducted on the integration of wave energy with desalination plants, very few studies were found and

only considering operation with a single WEC and very small desalination units [38–41]. The freshwater production that were considered ranged from laboratory scale [21], through 1.1 m³/day with the Del-buoy device [42] and 10 m³/day with an oscillating water column (OWC) device in India [43], to 300 m³/day using the inertial sea wave energy converter (ISWEC) developed in Italy [44]. Only the Perth wave energy project installed an array of three fully submerged buoys, supplying water and electricity to the Garden Island naval base (Australia) and reaching 150 m³/day [45]. The study done in 2016 by Franzitta et al., in Pantelleria (Sicily) with 51 WECs of the same DEIM point absorber (at development stage) to supply the total capacity of 3621.8 m³/day of two desalination plants, incorporates the concept of big scale wave farm [46,47]. Therefore, to our knowledge, only one work has been carried out considering large size desalination plants and using farms with a considerable number of WECs with high maturity level [48]. Nonetheless, the promising results obtained in that study have opened the way for further research on the possibility of making wave energy a cornerstone in the penetration of renewable energy in desalination plants situated near the coast. Other modeling and simulation studies that are based on analyzing the possibility to supply desalination plants with sea-water directly pressurized by the WECs (eliminating the cost and energy losses associated to electricity conversion) [49]; solve the concentration variation in the polarization layer in wave powered reverse osmosis [50]; or compare a wave energy-powered and wind-powered modular desalination system [51], confirm this possibility.

This work undertakes an inter-annual (multi-decadal) and intra-annual (monthly) study of two marine areas whose wave resources differ throughout the year with the intention of evaluating the behavior of four WECs that are at a high developmental stage. The aim is to determine whether the variation in WEC energy production depends more on the conditions of the marine area or on the device itself and how this variation affects desalination plant energy demand coverage.

The desalination plants selected use reverse osmosis (RO), the leading technology in the desalination market [19]. This technology has the advantage of modularity and scalability, as well as lower electricity consumption compared to thermal desalination systems. RO systems present a good and constant performance under continuous flow rate and feed pressure but the introduction of variable renewable energy sources poses challenging problems in this respect [52]. However, and although several authors have worked on renewable systems to supply RO plants operating under variable pressure and flow rate conditions [53], the advantage of wave energy within renewables is its better predictability and greater adaptability compared to other RE sources, ensuring less disruptive transmission [54].

In order to integrate all the factors discussed above, this work considers two pilot areas located in the northern and eastern coastal regions of Gran Canaria (Canary Islands, Spain). As they are in different areas, there are important differences in the behavior of the wave resource and the intra- and inter-annual variability. With this in mind, the objective is to analyze the performance of different WECs with high levels of technological maturity in order to select the optimal configuration of wave farms for two large size desalination plants situated near the selected pilot areas (two locations that are very different in terms of wave resource). A number of performance indicators are also identified and developed with the aim of facilitating the introduction of WEC technologies in the electricity coverage of desalination plants.

This work additionally aims to contribute to the implementation of wave energy in the energy mix of many regions in a short time period as possible. Climate change and its impact on coastal structures have been confirmed by several authors [42–44], and the application of WECs can not only contribute to mitigating climate change but also act as a possible protector of coastal areas [55–62].

2. Methodology

2.1. Pilot area selection

In order to carry out a realistic analysis and comparison, the first step is to find two coastal sea areas, close to which a large size RO desalination plant is contemplated or already in operation and whose wave resource differs in its main parameters (including, among others, significant wave height, peak wave period and wave power). In addition, all types of restrictions with respect to the sea area where the WECs would be installed have to be taken into account. Such restrictions may be due to the need for environmental protection (marine/land habitats, protected species, etc.), but can include other constraints such as submarine cable deployment, maritime routes, military areas, bathing areas, ports, etc., as well as technical restrictions such as bathymetric and seabed conditions.

2.2. Wave resource data acquisition and processing

An assessment of the wave energy resource is required to determine whether particular areas have highly diverse sea states. Data selection is vital for such an evaluation. As mentioned, long-term data series of over 20 years are highly recommended for interannual analyses. In the absence of equipment that provides real data (such as buoys), satellite data or resource maps are strongly recommended when looking for this type of data series.

In any research it is key to determine which kind of long series data are available. Within the Canary islands two types of series data are available: hindcasted data series (SIMAR) and bouys. The longest and widest available data are the time series of wave parameters from the coastal atlas of Spain called SIMAR points, provided by the Spanish Ports Authority (for more detailed information, please refer to [Appendix A](#)) [63]. These are modelled data that are available for a 61 year interval, up to 2018, with a frequency of 1 h. The bouys network (called REDCOS) includes several bouys with data available for a 26 year period, ending also in 2018 and with the same hourly frequency. This dataset has been validated by Losada et al., [64] and used by several authors [65–68] for other studies.

2.3. Simulation and processing tool

The R program, a language and environment for statistical computing and graphics, was used to process the dataset. R provides a wide variety of statistical (linear and nonlinear modeling, classical statistical tests, time-series analysis, classification, clustering, etc.) and graphical techniques, and is highly extensible [69]. Inside the program, the ggplot2 package was used as it contains the geom_density function designed to plot a smooth density estimate [70,71]. Using these features, we worked with the SIMAR and REDCOS datasets to evaluate the wave resource, obtaining scatter diagrams and other calculations such as seasonal wave direction frequency, wave power flux and mean monthly wave parameters conditions.

2.4. Wave energy converter selection

Many of the proposals for WECs have been abandoned, principally due to the scarcity of economic resources and subsidies that are needed to develop this technology on a commercial scale. The present research study focuses on devices of each classification range that currently have the highest technology readiness level (TRL). The overtopping Wave Dragon and the attenuating technologies of Waveston and Weptos were selected for this study due to their technological maturity (TRL values of 6 and 7 out of 9, implying the WEC prototype demonstration in a relevant environment). More information about these devices as their classification category and some technical information (company, location, water depth installation, generator capacity and TRL) can be

found in [Table 1](#) and in previous works from the authors [48].

2.5. Wave farm array configuration and energy production

When working with different areas, a fixed reference surface area will help for comparison purposes. In this case, and taking into consideration all environmental and technical restrictions in the selected pilot areas, a sea surface area of 8 km² was used as reference area. In addition, bathymetric conditions also need to be taken into account. In this case, a value of 200 m was selected as this has been used as the maximum depth in the general classification of typical WEC devices [26]. In addition, at greater depths the mooring system of the floating devices tends to be complex and difficult to install. A recent study confirmed that specific solutions are needed because conventional mooring configurations often do not provide suitable station keeping options [72].

In terms of WEC sizes or models, differences between wave climates of different areas favour the use of one or two sizes. In this case study, in order to make a comparison, the selected configurations and sizes correspond to the standard models that the companies of each technology have, using within these standards, those that are considered to have a better adaptability in the two studied areas based on the criteria of the converter developers. The 1.5 MW and 4 MW WaveDragon (W—D) could be used. Theoretically, the 1.5 MW version should adapt better to a lower wave climate decreasing its efficiency with long period waves [73]. The same principle applies to Waveston WECs. Two device sizes were simulated (one with an arrangement of 32 energy collectors (ECs) and the other with 50 ECs). The Weptos technology is modular and flexible, and so lends itself to scalability according to the wave climate, adapting the WEC to the reference area and achieving greater performance [74]. Making use of the laboratory scale, several sizes were tested using the Froude scaling law [54]. Scales 40/1 and 50/1 with 4 MW and 6 MW generator simulations were performed for both pilot areas, resulting in the selection of a 50/1 Weptos with a 4 MW generator as the optimum size for both pilot zones in terms of the capacity factor. [Table 2](#) shows the dimensions of all the devices selected for this study.

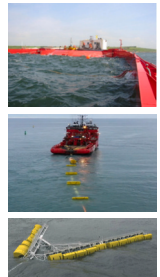
The next step is to configure the farm arrays. The key factors are the hydrodynamic interactions of the WECs, in terms of both near and far field effects [75]. Numerous investigations have been made in this regard. A detailed and chronological summary of these studies has been done in a previous work carried out by the authors [48]. Therefore, very few studies have considered the distance necessary for wave recovery between two aligned WECs. Because of all this, inter-distances (lateral and longitudinal) between WECs used in this study is based on the guidelines and technical specifications suggested by the WEC developers. These recommendations should allow q-factor values really close to 1 (defined q-factor as the ratio between the power output of an array on N units and the power output of N isolated units [37]), guaranteeing the technical and safety viability of the farms. One work on the overtopping Wave Dragon reported that at 3 km from the first row to the second one aligned to it (that is, the third staggered row in the wave farm) the incident wave power should be approximately equal [73,76]. In terms of Weptos, it is expected that each converter will have a watch circle with a diameter of roughly 1890 m [77]. In both cases, surface area and/or bathymetric limitations prevent placing a third and second row, respectively. As far as Waveston is concerned, the longitudinal extension of its devices prevents the placement of a second row, so the farm is configured by deploying the WECs parallel to each other and perpendicular to the predominant wave direction [74]. [Table 2](#) also showed lateral and longitudinal distances established between each WEC in the corresponding wave farm array configuration.


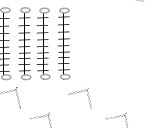
Energy production was calculated using the power matrixes of each WEC provided by the technology developers (which relate power generation to a given sea state condition as defined by H_s and T_p). The product of the power matrix with the scatter diagram of the pilot area (which shows the probability of occurrence of the different sea states

Table 1
Wave energy converter selection.

	Company	Type	Location	Depth (m)	Capacity (MW)	TRL
Wave Dragon	Wave Dragon Ltd	Overtopping	Offshore	> 30	1.5; 4; 7 and 12	7
Wavepiston	Wavepiston	Attenuator	Offshore	20–100	0.1–0.4	6/7
Weptos	Weptos A/S	Attenuator	Offshore	40–80	4–6	6

Table 2
Wave energy converter dimensions and farms configurations.

WEC	Width [m]	Length [m]	Height [m]	Picture Ref [78–80]
Wave Dragon [1.5 MW]	152	96	12	
Wave Dragon [4 MW]	230	150	16	
Wavepiston [32 EC]	9	240 ^a	4	
Wavepiston [50 EC]	9	370 ^a	4	
Weptos	12	472.5	10	

Wave farm configurations				
WEC	Array configuration	Lateral distance [meters]	Longitudinal distance [meters]	Picture
Wave Dragon [1.5 MW]	Staggered	304	130	
Wave Dragon [4 MW]	Staggered	460	130	
Wavepiston [32 EC]	Aligned	60	N.A	
Wavepiston [50 EC]	Aligned	60	N.A	
Weptos	Staggered	945	945	

^a In the case of Wavepiston, the length of the device is understood as the length assuming the set of energy collectors. Each energy collector (EC) is 4 m long.

represented by the bivariate distribution of H_s and T_p) gives the energy production [73,74,77]. It should be noted that the effect of wave direction has not been taken into account in the calculations. Both Wave Dragon and Weptos WECs are not significantly affected by this parameter, but this is not the case of Wavepiston since it is a direction-dependent WEC. Therefore, in areas where the dispersion in the direction of the resource is important, the annual energy production may be slightly overestimated.

2.6. Performance indicators

In order to evaluate the adaptability, electricity coverage, stability and efficiency of wave farms coupled to desalination plants, a series of performance indicators were defined and estimated. The first indicator, the WEC-resource pairing parameter, indicates the adaptability of the different WECs to the wave resource available in the coastal area where the desalination plant is located. This parameter greatly affects the efficiency and stability of electricity production.

Once the adaptability of the WEC to the resource and its corresponding electricity production has been found, the percentage of desalination plant electricity demand coverage can be estimated. This second indicator not only quantifies but also aims to analyze the stability of the wave farm in terms of electricity production with respect to the possible energy peaks and troughs of the desalination system.

Other important indicators when deciding the best wave farm are based on the surface area available for possible deployment. Once an area has been determined that complies with environmental and other restrictions, the technical parameters of each WEC technology, such as its minimum and maximum bathymetry, its inter-WEC spacing (both

lateral and longitudinal distances) and its safety distances must be taken into account. These parameters will determine the surface area occupied by the corresponding WEC technology.

Supported by the parameters set out in subsection 2.5, the energy density indicator is predefined with the intention of evaluating which farm provides the highest annual energy production per occupied square meter. Also, as the wave resource is typically considered to be a linear resource and is defined by the length of the wave farm, another metric shows the farms energy production per meter of wave length.

Likewise, and for the specific case of coupling with desalination plants, the final indicator shows the surface area occupied by each WEC technology to obtain one cubic meter of freshwater.

3. Study cases and pilot areas selection

The island of Gran Canaria is part of the Canary archipelago. These islands constitute one of the outermost regions of the European territory and, consequently, highlight the high dependence on water and energy from external territories required to satisfy their own needs [24]. However, these particular islands are characterized by having very favorable endogenous conditions for the implantation of renewable technologies (high average wind speeds, high solar radiation) [81–85]. The energy policies that have been established contemplate a sustainable and fruitful transition to the goals set for 2030 and 2050 [86,87]. Surrounded by the Atlantic Ocean, wave energy has a place in this new scenario. Several studies conducted on the islands in relation to the wave resource corroborate this [67,88–90]. In addition, along the Canary coast there are a large number of desalination plants which can potentially benefit directly from this resource [48,68]. Following the steps

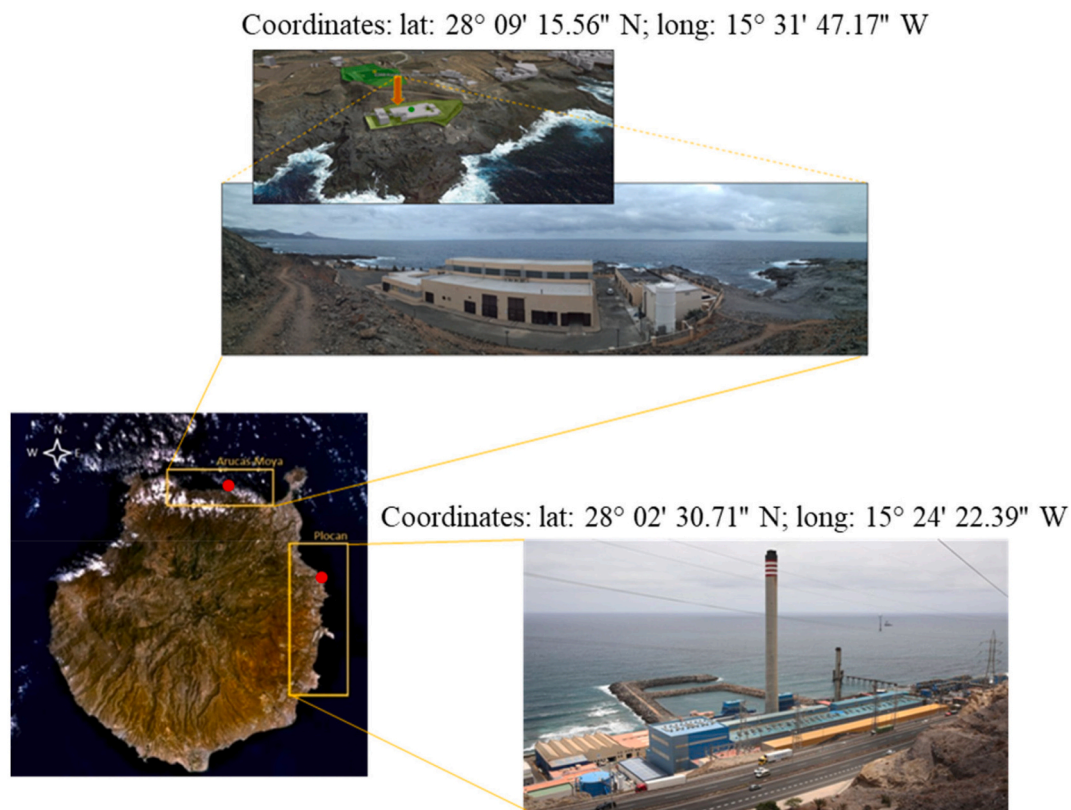


Fig. 1. Selected pilot areas.

described in the methodology (Section 2.1), two pilot areas (north and east of the island), which show a remarkable difference in terms of wave resource (the north area doubles the potential of the east one), were selected. In both cases, none of the environmental or technical constraints are compromised, being areas available for the installation of this type of marine renewable and next to a large reverse osmosis desalination plant in operating. Fig. 1 shows the selected pilot areas in a map of Gran Canaria.

3.1. Arucas-Moya pilot area

The Arucas-Moya (A-M) region is located in the north of Gran Canaria. It is characterized by having the highest wave power of the entire island (annual average of 19.3 kW/m). The terrestrial perimeter of the selected coast has scattered settlements in small villages, some agriculture areas and a desalination plant. Plant size is average in relation to the other desalination plants located throughout the island.

With a desalination capacity of 15,000 m³/day, the plant employs the RO process. Its specific consumption (3.84 kWh/m³ for desalination and 4.20 kWh/m³ for desalination and initial pumping distribution) results in an electricity demand of 19 GWh/year. In the simulation, the WEC farm is installed in the neighbouring waters [91].

The analyzed area is 8 km², with a bathymetric range between 20 and 200 m. However, the depths in the vast majority of the area exceed 50 m. The seabed is mostly rocky block-type substrate, although sedimentary substrate like sand is also found [92].

To study the wave resource, the 4,035,011 SIMAR point has been selected since it is close to this pilot area. The depth of seabed at this SIMAR point (50 m) is similar to the average depth of the pilot area.

3.2. PLOCAN pilot area

The oceanic platform of the Canary Islands (PLOCAN) is located east of the island of Gran Canaria. In this location, the wave resource is much

lower (annual average of 5.6 kW/m). However, this public domain marine area provides the scientific, institutional and business community with unique opportunities to support deep sea activities with sufficient environmental guarantees and within a stable regulated framework [93]. The marine test site covers the same size area as the A-M pilot area (8 km²) and the maximum depth is 200 m. The predominant substrate is sand (94.2%) [94].

As there are two water treatment plants near the test area (a desalination plant and a wastewater treatment plant, last one with a specific consumption of 1.7 kWh/m³), as well as a shopping center, the electrical connection possibilities are very favorable [93]. The seawater RO desalination plant (Las Palmas III), with a capacity of 65,000 m³/day [95], is responsible for supplying potable water to around 500,000 people [96]. The energy demand in 2019 amounted to 91,037 MWh [97], resulting in a specific consumption of about 3.84 kWh/m³.

To study the wave resource in this pilot area, the Triaxys buoy (REDCOS point 1414) at 30 m depth was selected.

4. Results

This section presents the results of the research applied to the practical case of the island of Gran Canaria, once the pilot areas have been selected in Section 3. It starts with a detailed analysis of the wave resource in both pilot areas, ending with an analysis of the performance indicators proposed in Section 2.6.

4.1. Wave energy resource

4.1.1. Arucas-Moya pilot area

Fig. 2 shows the scatter diagrams of (a) the mean annual peak wave period (T_p) vs. significant wave height (H_s) values for the selected SIMAR as well as the same mean values for the two months (June (b) and January (c)) with the most extreme values. As can be observed, the wave resource distribution varies considerably between the two months. As a

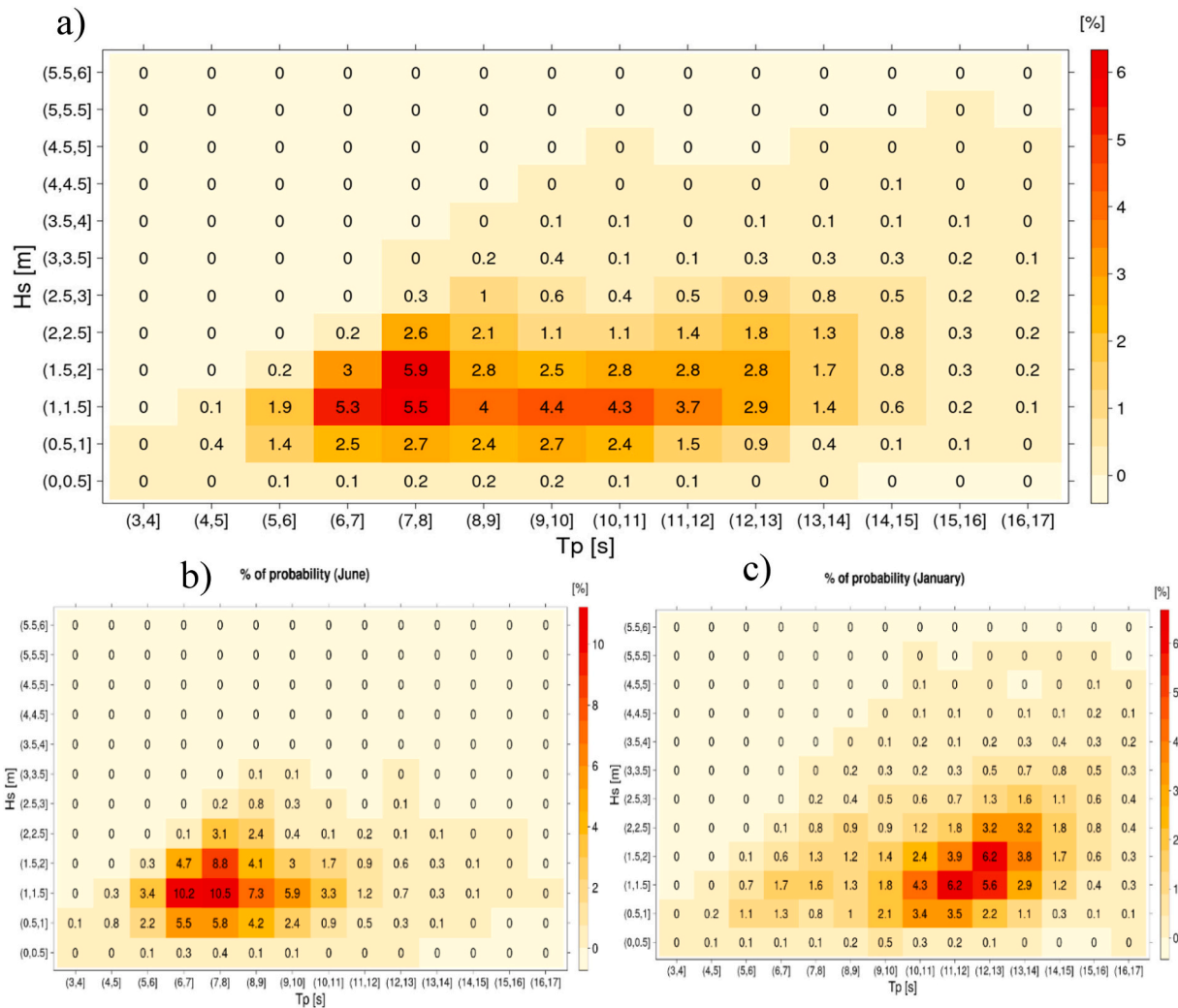


Fig. 2. Scatter diagrams showing the mean annual a) and mean June b) and January c) peak wave period (T_p) vs. significant wave height (H_s) values in the Arucas-Moya pilot area. The sidebar shows the colour scale for the probability of occurrence in percentage (%).

Table 3
Monthly wave energy conditions and wave power in the Arucas-Moya pilot area.

Month	Significant wave height [m]	Peak wave period [s]	Main wave direction [°]	Wave power [kW/m]
January	1.696	11.551	247.415	19.019
February	1.723	11.045	221.420	18.583
March	1.762	10.763	212.367	17.804
April	1.648	9.742	182.885	14.017
May	1.488	8.992	152.507	10.247
June	1.344	8.038	104.163	7.225
July	1.588	7.588	36.689	9.483
August	1.500	7.734	49.810	8.544
September	1.323	8.959	141.312	8.034
October	1.470	10.307	223.580	12.400
November	1.623	10.661	211.207	15.882
December	1.663	11.238	224.062	17.983

first observation, the probability of keeping a sea state with a higher degree of constancy is 69.35% higher in the month of June than in January. However, significant wave height and peak wave period show lower values in June. Since wave energy potential (wave power) depends to a large extent on both parameters (H_s and T_p) [98], it was therefore decided to undertake an in-depth analysis of intra-annual variability to facilitate the understanding of the wave pattern and the optimization of the wave farm configuration. Table 3 shows the mean

values of H_s , T_p , main wave direction and wave power (P) for each month calculated with Eq. (1) where g is the gravitational acceleration (9.81 m/s^2), ρ the seawater density ($\sim 1.027 \text{ kg/m}^3$) and T_e is the energy period which has been calculated from the peak period of the dataset assuming the Jonswap spectra ($T_p = 1.12 T_e$) [99].

$$P \text{ [kW/m]} = \frac{\rho g^2}{64\pi} T_e H_s^2 \tag{1}$$

In the specific case of the north of Gran Canaria, the maximum variation between heights is 33%, while in the case of the peak period parameter this value is 52%. This situation indicates the degree of importance of local weather conditions such as wind strength in the generation of the wave resource. The greatest wave energy potential is found in the winter season (December, January and February) which is in line with the highest H_s and T_p values (see Table 3). These values are due to swell (defined as 10 s or more of wave peak period) originating a highly energetic wave environment. In contrast, the months with the lowest wave energy potential are the summer months of June, July, August and September. During this season, the island's weather is characterized by the presence of the trade winds, the permanent east-to-west prevailing winds that flow in the Earth's equatorial region (between 30°N and 30°S latitudes). In the Canary Islands, the trade winds follow a diurnal pattern similar to that of the sea breeze. They are characterized by having a higher wind intensity during the warmest hours and in the afternoon,

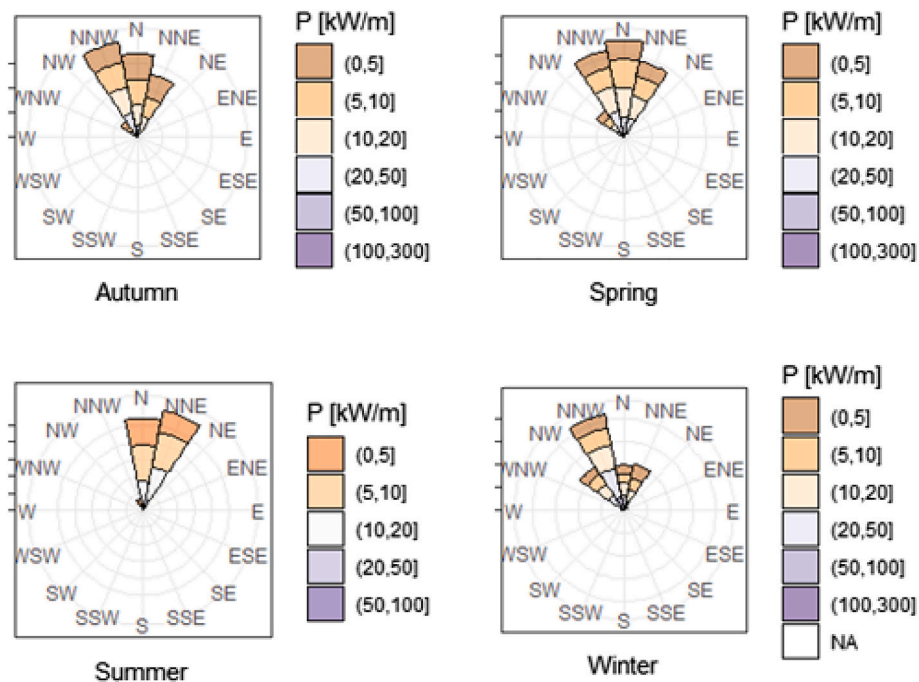


Fig. 3. Seasonal wave direction frequency and wave power flux in the Arucas-Moya pilot area.

increasing in intensity during the summer period.

Using a 10 s period as an approximate point of separation between wind-wave and swell [100], it can be argued that the wave peak period in summer, and part of spring, is being originated by wind (see Appendix B). This distribution again shows the seasonality of the wave resource in the north part of the island. During the winter, direct swell from the Atlantic Ocean leads the wave pattern (that comes from propagating over thousands of kilometers across entire ocean), while in summer the geographical disposition of this coast does not favour the trade winds, thus it is not possible to maintain the balance in the energy potential throughout the year.

This situation should be a priority when selecting the WEC, since the technology must take advantage of the wave resource throughout the year. Greater adaptability to a wide range of sea states will guarantee higher energy production.

A seasonal evaluation of the wave resource including the wave direction is shown in Fig. 3. The predominant direction of the waves varies considerably from winter to summer. The wave resource is not unidirectional. Although in summer it remains more constant, coming from the northeast and matching the trade winds (carrying less wave energy potential). In contrast, in winter, influenced by swell waves of the Atlantic with a more energetic wave, the main wave direction is the northwest. In spring and autumn, a combination of the prevailing winter and summer wave directions can be observed, although the wave energy potential in autumn is slightly higher due to a greater swell influence than in spring.

4.1.2. PLOCAN pilot area

Although located in the same island, the wave resource in the PLOCAN pilot area differs greatly from the one in Arucas-Moya area (approximately 130% less than the annual mean wave energy potential in the northern zone). In this case, the most extreme months of the year are October and February. Fig. 4 shows the scatter diagrams of the (a) mean annual peak wave period (T_p) vs. significant wave height (H_s) values for the REDCOS point and the same values for the two most extreme months (October (b) and February (c)).

In this area, a greater variation occurs in the significant wave height while the peak wave period remains much more constant. Table 4 shows

the mean values of these parameters and of the wave direction and wave power for each month of the year. It can be seen that the months with the highest wave energy potential are February, July and March, but with no significant differences. Therefore, in this case, seasonality is not present. Likewise, there is no contribution from swell (above 10 s of wave peak period), and hence it has a less energetic wave.

It should also be noted how the influence of the trade winds is all year round on the east coast of the island, with wind-swell (under 10 s of peak wave period) as opposed to swell observed most of the time. This is due to the shadow of the island itself impeding the swell contribution while, at the same time, the orientation of the site coincides with the main direction of the trade winds.

This whole situation contributes to the fact that the seasonal wave resource study shows a low but relatively constant wave energy potential is obtained throughout all the seasons (matching the trade winds) as shown in Fig. 5. Thus, there is no appreciable seasonal variation. Likewise, the direction of the resource is practically constant (from the northeast) throughout the year.

This unidirectionality in the wave direction, strengthens the installation of direction-dependent WECs, which can also cover a narrow bandwidth in terms of sea states due to the homogeneity of the resource on an annual basis.

The differences between the wave climates on both coasts points out at the possibility that the WECs may behave differently in each pilot zone. Although the Arucas-Moya area shows a higher energy potential, its higher seasonal variation may appear as a weakness when it comes to taking advantage of that energy. Likewise, the east coast within the PLOCAN area shows a lower resource, which, even though it is uniform (it shows a 69% greater probability of reproducing the same sea states during the year), may be insufficient to produce the electricity needed to cover the desalination plant electricity demand. The wave resource analysis outlines some indications, highlighting the clear need to carry out a WEC-resource pairing assessment for each technology for a suitable selection.

Finally, in terms of inter-annual variations, analyzing the period 1992–2018 in both areas it can be seen that there is no progressive increase in the mean H_s , mean T_p or maximum H_s parameters over time. There is also no correlation in the variation of the parameters (the H_s

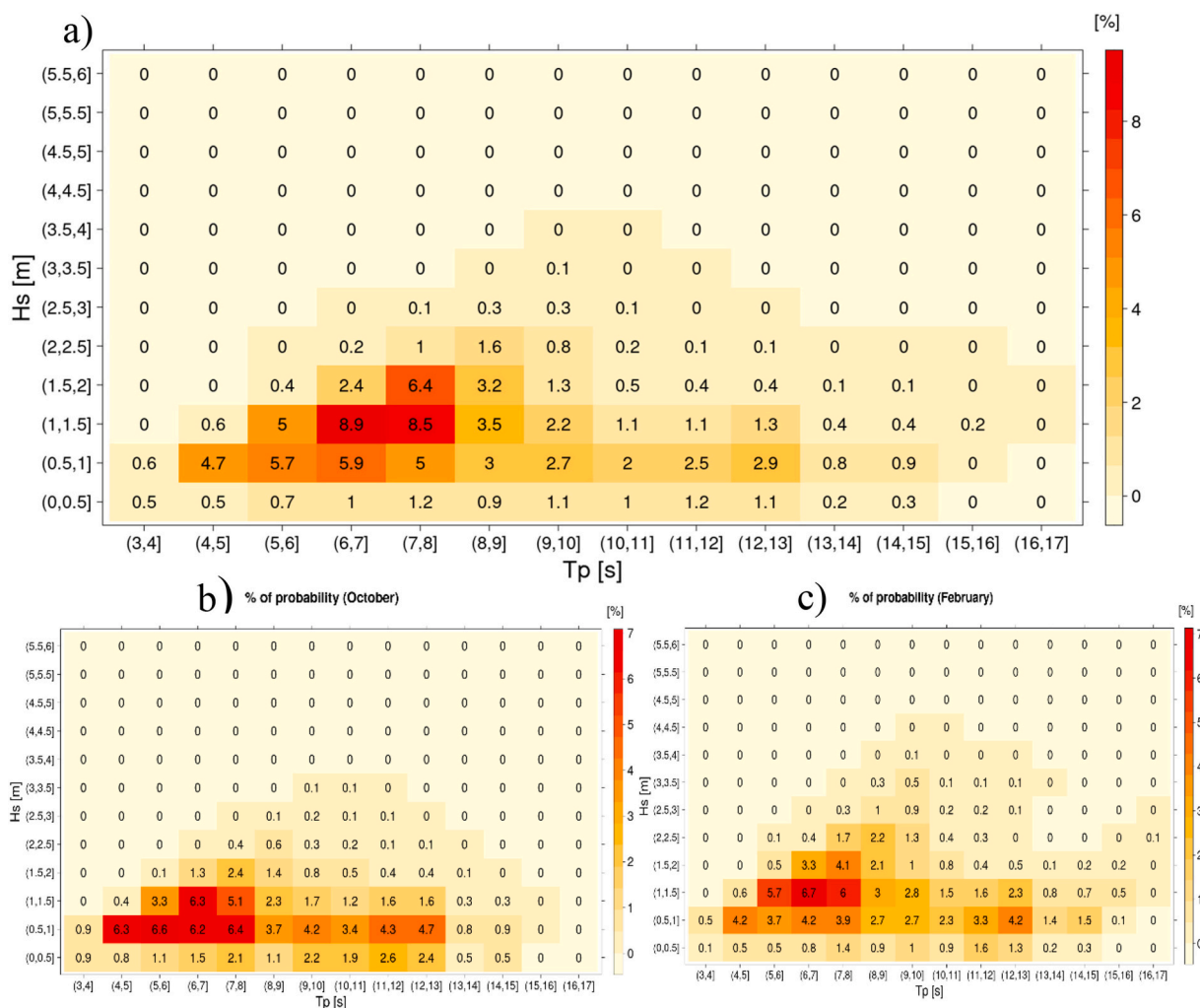


Fig. 4. Scatter diagrams showing the mean annual a) and mean October b) and February c) peak wave period (T_p) vs. significant wave height (H_s) values in the PLOCAN pilot area. The sidebar shows the colour scale for the probability of occurrence in percentage (%).

Table 4

Monthly wave energy conditions and wave energy potential in the PLOCAN pilot area.

Month	Significant wave height [m]	Peak wave period [s]	Main wave direction [°]	Wave power [kW/m]
January	1.172	8.994	-73.7142	6.557
February	1.236	8.651	-71.8989	7.236
March	1.187	8.767	-72.4410	6.559
April	1.624	8.100	-72.1971	5.843
May	1.110	7.698	-73.4938	5.221
June	1.143	7.111	-73.3568	4.947
July	1.393	7.279	-70.8540	6.997
August	1.129	7.128	-70.5918	5.951
September	1.043	7.386	-73.5535	4.157
October	0.950	8.410	-71.1713	4.063
November	1.178	8.867	-73.1322	6.518
December	1.102	8.912	-72.6406	5.719

and T_p do not vary in a similar way). In both areas, the most noticeable annual variation occurs in the maximum H_s data (with a variation of 68% between 2012 and 2013 in Arucas-Moya and 48% between 1992 and 1993 in PLOCAN). This parameter is followed by the variations in mean H_s with a maximum difference of 22% in PLOCAN and 10% in Arucas-Moya and the mean T_p with variations of 7–10% in both zones. The data used for this evaluation are included in Appendix C. The multi-decadal study showed no significant variations over the years that could

lead to long-term under-dimensioning of a WEC farm in either area (Table 5).

In terms of the maximum significant wave height, the percentage of variation does not exceed 25% in either pilot area. The A-M pilot area has a more pronounced inter-decadal variation in the peak wave period parameter, while the PLOCAN area shows a higher rate of variation in the significant wave height parameter, although in both cases the variation is below 12%.

4.2. Wave farm array configuration and electricity production

The maximum number of WECs per farm was determined on the basis of the dimensions of the WEC and the required inter-space distances (explained in the methodology section), obtaining the following results:

- 1.5 MW WaveDragon: eight WECs in the first row and seven in the second.
- 4 MW WaveDragon: five WECs in the first row and five in the second.
- 32/50 EC Wavepiston: fifty WECs in a single row.
- Weptos: three WECs (50/1 with a 4 MW generator) in a single row.

Table 6 summarizes the electricity produced by a single device, and the producible electricity in each farm using the maximum number of WECs that can be placed within the pilot areas.

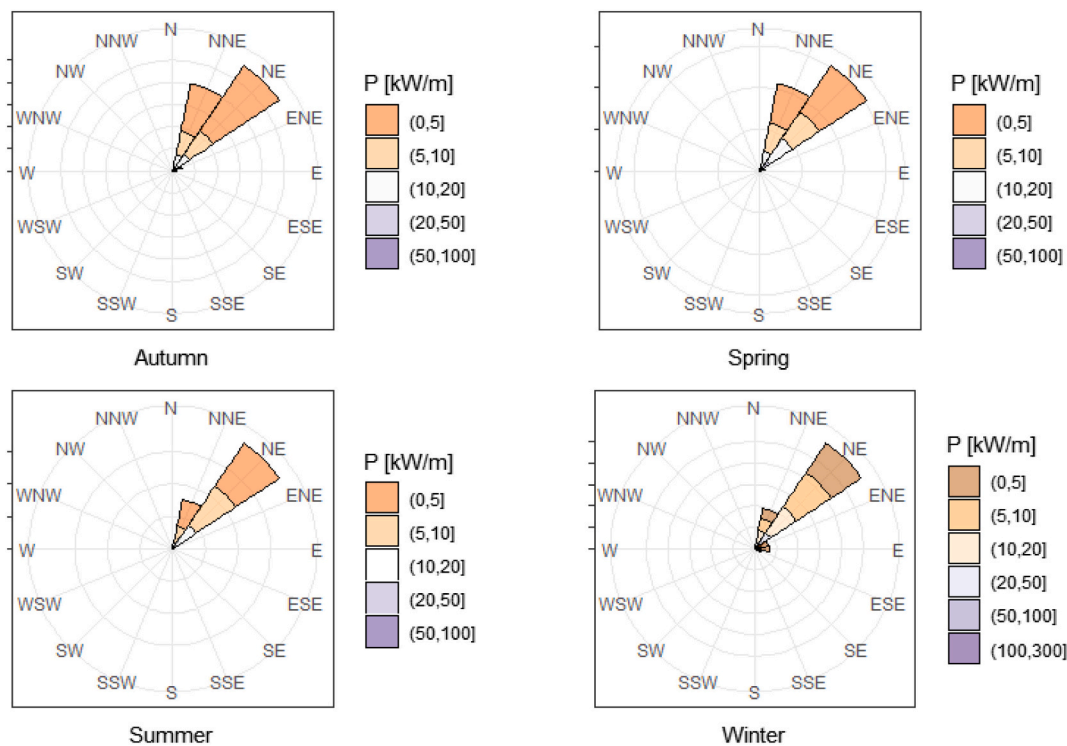


Fig. 5. Seasonal wave direction frequency and wave power flux in the PLOCAN pilot area.

Table 5
Multi-decadal study of significant wave height and wave peak period in the Arucas-Moya and PLOCAN pilot areas.

Decade	Arucas-Moya			Decade	PLOCAN		
	Mean H_s (m)	Mean T_p (s)	Max H_s (m)		Mean H_s (m)	Mean T_p (s)	Max H_s (m)
1958–1968	1.59	9.59	6.07				
1968–1978	1.54	9.42	6.56				
1978–1988	1.56	9.59	5.29				
1988–1998	1.59	9.66	6.58	1992–2002	1.14	8.15	4.9
1998–2008	1.58	9.74	5.81	2002–2012	1.12	8.05	4.4
2008–2018	1.55	10.21	6.20	2012–2018	1.25	8.08	4.7

Table 6
WEC farm electricity production analysis.

WEC	Electricity production of a single device [MWh/year]		Max. number of WECs in the reference area	Electricity production of wave farm [MWh/year]	
	Arucas-Moya	PLOCAN		Arucas-Moya	PLOCAN
WaveDragon (1.5 MW)	2100	1503.4	15	31,500	22,551
WaveDragon (4 MW)	5311	2894.6	10	53,310	28,946
Wavepiston (32 EC)	545	634	50	27,250	31,700
Wavepiston (50 EC)	681.4	944.6	50	34,070	47,230
Weptos	6015	3942	3	18,046	11,826

Table 6 shows important differences in the amount of electricity production among the different single devices. However, analyzing this relationship under the farm configuration, it can be observed that this production ratio begins to homogenize. Since the occupied surface is the same in all cases, the possibility of including a higher number of devices of the smaller technologies (which also show a lower single power),

makes them competitive against the bigger ones (higher single power). Moreover, the different technologies differ also in the electricity production, some of them are more productive in the northern part of the island, while other reach higher production values in the eastern area. This point confirms the hypothesis made in Section 4.1 (WECs may behave differently in each pilot zone) and highlights the need to develop performance indicators that speed up the optimization process to find out the most suitable technology for each zone/wave resource.

4.3. Performance indicators

The indicators explained in Section 2.6 were applied and evaluated in both pilot area locations.

4.3.1. WEC-resource pairing

The results for WEC and wave farm electricity production in Table 6 show the mean annual values, but do not show the effects of the temporal variability of wave energy on the power that can be supplied to the desalination plant. The WEC-resource pairing indicator is an important tool in this respect. A monthly study of the electricity production of each WEC was therefore carried out to verify the adaptability of each device and determine the most suitable type for each area.

Fig. 6 shows the monthly wave farm electricity production for the A-M pilot area. As can be seen, the device with the highest electricity

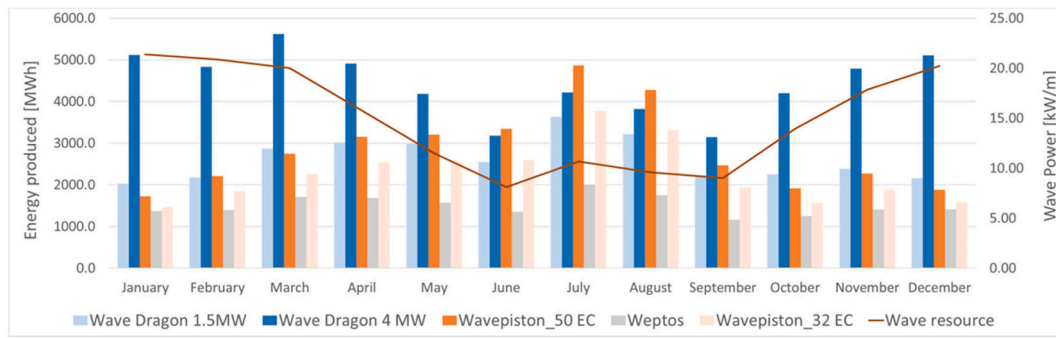


Fig. 6. Wave farm electricity production in the Arucas-Moya pilot area.

production in this area, and which also shows a generation profile similar to that of the wave resource throughout the year, is the 4 MW Wave-Dragon. However, the month with the highest wave resource (January) does not correspond to the month with the highest electricity production (March), which indicates that this device largely depends on wave height as its highest value (1.76 m) occurs in this latter month. This situation is confirmed again in the opposite case, where the lowest electricity production with this WEC occurs in the month with the lowest significant wave height, September (1.32 m). This is due to the configuration of the WEC, which has a ramp on its front face, which is the wave entrance. Behind the crest of the ramp there is a tank that stores the water that overtops the ramp. Energy is extracted as the water storage in the tank flows back to the sea through hydro turbines. The higher the waves are, the easier it is for the water mass to circulate through them. In the case of the overtopping 1.5 MW Wave-Dragon, its best scenario contemplates wave heights above 1.5 m and peak wave periods of around 7 and 8 s. Its optimal operation in smaller waves is due to the height of the ramp and of the device itself being lower than the 4 MW Wave-Dragon.

In the case of Wavepiston, both configurations (32 and 50 EC) follow the same pattern, differing in the degree of electricity production by the number of collectors. However, the electricity profile produced is in complete contrast with that of the wave resource, confirming that not all WECs have an optimal point when they are located in an area with high wave energy potential. Lastly, the Weptos wave farm has a lower electricity production, but also has the advantage of a much more constant production throughout the year. In this respect, its stable behavior favourably matches the electricity demand of a desalination plant.

This situation varies drastically if only one device of each technology is considered. It can be seen in Fig. 7 how the 4 MW Wave-Dragon and the Weptos devices lead electricity production, and although the Wave-Dragon device again maintains a behavior very similar to that of the wave resource, the Weptos device manages to contribute 13% more electricity over the course of the year. It is also clearly seen that a farm

installation in the case of the Wavepiston device is completely necessary to allow a significant percentage of electricity to be supplied to the desalination plant.

From the perspective of the PLOCAN scenario, Fig. 8 shows the performance of the selected WEC farms. In this case, the Wavepiston 50 EC device heads the electricity production, followed at some distance by the Wave-Dragon 4 MW (contributing 55% less electricity). In addition, all the technologies tend to maintain a behavior similar to that of the wave resource. This is because the resource in this area is characterized by a narrow wave distribution climate which is characterized by low periods (which explains the high performance of the Wavepiston device).

Furthermore, compared to the Arucas-Moya pilot area, which has a broader wave direction range, the main wave direction in the PLOCAN pilot area remains much more constant. Consequently, devices that depend on wave direction like Wavepiston (fixed anchored), and need to have their plates facing the wave crest, do not have an overestimation in the annual energy production calculations. Likewise, the increase in the capacity factor by 28% in Wavepiston 50 EC confirms that the energy extraction system of these devices adapts much better to the PLOCAN sea conditions than the Arucas-Moya pilot area. On the other hand, the dependency on wave direction of the electricity production of the Weptos and Wave-Dragon devices is negligible given their structural arrangement (modularity in the case of Weptos and deflectors in the case of Wave-Dragon) as well as their anchoring configurations. The main cause of the reduction in electricity generation is the better match to an area where the wave resource is more energetic (higher wave height and period values).

Comparing both locations quantitatively at farm level, it can be confirmed that the devices that produce the highest amount of electricity in the northern pilot area (4 MW Wave-Dragon) reduces its electricity production by 83.5% when located in the eastern pilot area of the island; while the device that produces the highest amount of electricity in the PLOCAN area (Wavepiston 50 EC) reduces its electricity

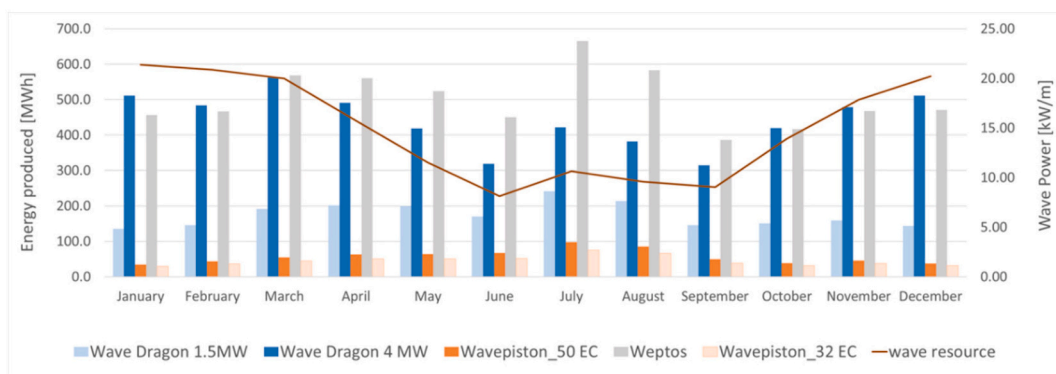


Fig. 7. Single WEC device electricity production in the Arucas-Moya pilot area.

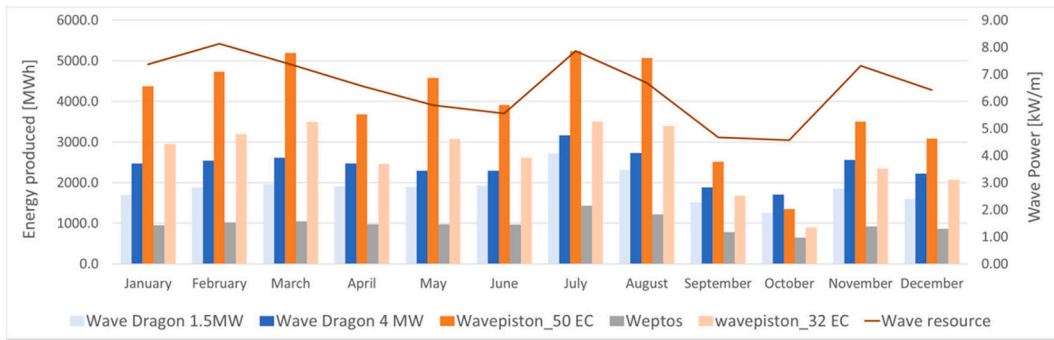


Fig. 8. Wave farm electricity production in the PLOCAN pilot area.

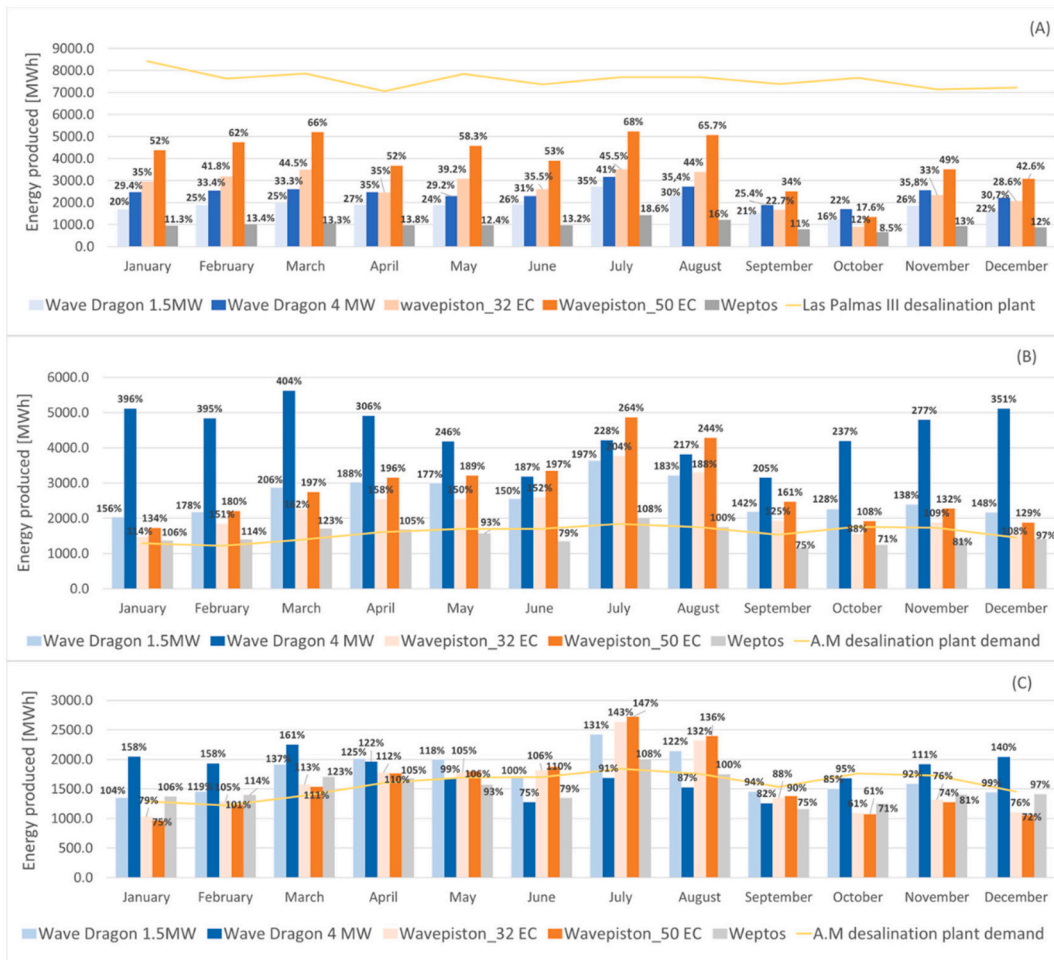


Fig. 9. Monthly wave farm electricity production vs. desalination plant electricity demand in the Arucas-Moya and PLOCAN pilot areas. A) PLOCAN wave farm electricity production vs. Las Palmas III desalination plant electricity demand; B) Arucas-Moya wave farm electricity production vs. Arucas-Moya desalination plant electricity demand; C) Arucas-Moya electricity production needed by each farm vs. Arucas-Moya desalination plant electricity demand.

production by 16.3%. Therefore, devices designed for high wave potentials may suffer a considerable loss of efficiency when operating in low energy sites.

4.3.2. Electricity demand coverage

The percentage of electricity demand coverage when the WEC system is coupled with a desalination plant is the next indicator evaluated. Fig. 9 shows the behavior of each technology against the electricity demand of the two plants in the pilot areas. The Las Palmas III plant consumes approximately 5 times more electricity than the Arucas-Moya

plant, and considering the same sea surface area to implement the farms, it is logical that the percentage of electricity coverage will differ considerably between the two areas.

In the case of Las Palmas III none of the wave farms can meet the annual electricity demand (a consequence of the limited deployment area in comparison to the desalination plant size); the Wavepiston (50 EC) WEC farm shows the highest electricity annual coverage (52%), although it never fully meets the demand for any month of the year. The opposite case is found in the north of the island, at the Arucas-Moya plant, where the only wave farm that is unable to meet the annual

demand uses the Weptos technology (a consequence of the space needed for its deployment). In the other wave farm types, a considerable reduction in the number of devices (about half for each farm) would be possible while maintaining the certainty of covering the annual electricity demand of the desalination plant (Fig. 9-C). In this sense Arucas-Moya wave farms can be reduced from 15 to 10 WECs in 1.5 MW Wave Dragon; from 10 to 4 WECs in 4 MW Wave Dragon; and from 50 to 28 WECs and 50 to 32 WECs in Wavepiston 50 EC and 32 EC respectively.

Unlike the constant behavior of the electricity demand of the desalination plant, wave energy, like the vast majority of renewable energies, displays fluctuations that have to be managed to ensure the electricity demand can always be met. Nonetheless, the degree of this variation is not the same for all devices. A monthly analysis shows that the energy coverage in percentage terms for most of the technologies show higher seasonal differences in the PLOCAN pilot zone than in the Arucas-Moya area. As shown in Fig. 9, the WEPTOS and Wave Dragon devices show less variations in percentage terms throughout the year at both sites and, thus, less variations in the percentage of demand supplied. As an example in the PLOCAN area, the highest monthly variation of the Wavepiston technology (50 EC) is as high as 275% while for the 4 MW Wave Dragon farm this value reaches 86%. Likewise, in Arucas-Moya the highest monthly variation of the Wavepiston (50 EC) reaches 144%, while for the WEPTOS and 1.5 MW Wave Dragon these values are 72% and 62% respectively.

All of the above confirms that, when analyzing wave energy as a potential renewable energy for its introduction into desalination plants, the study cannot solely focus on the implementation of a single device. The behavior of wave farms and their configuration based on the available space and the necessary safety distances between them to ensure that there are no interactions that affect the energy production are also crucial factors.

4.3.3. Energy density

In order to compare the wave farms in each of the pilot areas, parameterized performance indicators (like the energy density per device/farm or the surface area occupied by the wind farm to obtain one cubic meter of freshwater) are needed which are independent of the desalination plant demand. Table 7 shows the energy density values per device and farm.

In the Arucas-Moya pilot area in terms of single devices, the Weptos technology provides the highest value of energy density (1.06 MWh/m²). However, when considering a Weptos wave farm, this value decreases enormously as the system requires long safety distances due to its type of movable anchorage and its versatility in adjusting to the direction of the incoming wave and, thus, this wave farm shows the lowest energy density figure. Table 7 shows that, although in terms of single device the energy density figures are very different among the wave devices, in terms of wave farm the energy density figures are much more similar. In the PLOCAN pilot area a similar trend can be observed but in line with the variations previously shown by the different technologies in lower wave resource environments, where the Wavepiston device shows a better behavior, which is directly translated in higher energy densities in terms of single device as well as in terms of wave farm, and the other technologies show a lower performance.

Table 7
Annual energy density per device & farm for the Arucas-Moya and PLOCAN.

WEC	Annual energy density per device [MWh/m ²]		Annual energy density per farm [MWh/m ²]	
	Arucas-Moya	PLOCAN	Arucas-Moya	PLOCAN
Wave Dragon (1.5 MW)	0.143	0.103	0.033	0.023
Wave Dragon (4 MW)	0.141	0.077	0.032	0.017
Wavepiston (32 EC)	0.252	0.293	0.035	0.040
Wavepiston (50 EC)	0.205	0.283	0.028	0.039
Weptos	1.060	0.695	0.025	0.016

Table 8
Comparison of the annual energy production per meter of wave crest.

WEC	Annual energy production per meter of wave crest [MWh/m]	
	Arucas-Moya site	PLOCAN site
Wave Dragon (1.5 MW)	9.4	6.7
Wave Dragon (4 MW)	15.7	8.6
Wavepiston (32 EC)	8.3	9.6
Wavepiston (50 EC)	10.4	14.4
Weptos	6.3	4.1

Table 9
Annual freshwater production per WEC device and farm vs. covered area.

WEC	Freshwater produced per device [m ³ /m ²]		Freshwater produced per farm [m ³ /m ²]	
	Arucas-Moya	PLOCAN	Arucas-Moya	PLOCAN
Wave Dragon (1.5 MW)	37.4	26.8	8.7	6.2
Wave Dragon (4 MW)	36.9	20.1	8.4	4.6
Wavepiston (32 EC)	65.7	76.4	9	10.5
Wavepiston (50 EC)	53.3	73.9	7.3	10.1
Weptos	276.3	181.1	6.4	4.2

4.3.4. Energy production per meter of wave length

The standard unit of wave energy production relate the energy produced by the converters to the wave length. The performance indicator that shows this relation is shown in Table 8, which allows a comparison among the different devices in terms of energy production.

Table 8 shows that the 4 MW Wave Dragon reaches the highest annual production rate in the Arucas-Moya site while Wavepiston does so in the PLOCAN site.

Last column of Table 8 shows the percentual difference in terms of energy production of each farm between the two different locations.

4.3.5. Freshwater production vs. covered area

This section compares the freshwater production that each technology is capable of contributing per square meter of covered surface area. In order to perform the calculation, the value of the specific consumption of each plant is used, which in this case is 3.84 kWh/m³ for both plants, a value that is within a standard global range. Table 9 shows the mean annual results.

As expected, the differences are very high in terms of single devices for both sites, being clearly Weptos the technology with the highest performance in terms of freshwater production per surface unit. Nonetheless, at farm level the differences are not as high as in terms of single devices, especially in the higher wave resource area. The differences are higher in the lower wave resource area, the PLOCAN one, where the Wavepiston adapts better. The results are in line with those obtained for the energy density in the different configurations and areas.

5. Conclusions

This work analyses the potential exploitation of WEC farms in medium wave climates as energy suppliers for desalination plants. For this purpose, a series of performance indicators was developed in order to analyze the adaptability of wave farms to wave resources, the stability of electricity production with respect to the desalination plant electricity demand profile and the percentage of electricity coverage, among others. With the intention of being able to use the indicators for any desalination plant, some indicators were parameterized, facilitating knowledge of electricity production and/or cubic meters of freshwater production per square meter of covered sea surface.

To evaluate the consistency of these indicators, they were applied to two maritime areas with different sea states and wave patterns, within the medium wave energy potential range. The northern and eastern

coasts of the same island (Gran Canaria, Spain) were used as a practical case study. The first pilot area (northern coast) is characterized by a higher wave resource potential, higher seasonality and strong variations in the predominant direction of the waves from winter to summer. In comparison, the second pilot area (eastern coast) is characterized by a lower resource potential, low seasonal effect and unidirectional waves. This unidirectionality in the wave direction, favours the installation of direction-dependent WECs, which can also cover a narrow bandwidth in terms of sea states due to the homogeneity of the resource on an annual basis. The analysis of the different wave climate sites confirms that the WECs behave differently in each pilot zone. Nonetheless, the degree of this variation is not the same for all devices. Although the northern area shows a higher energy potential, its higher seasonal variation may appear as a weakness when it comes to taking advantage of that energy. A monthly analysis shows that the electricity coverage in percentage terms for most of the technologies show higher monthly differences in the PLOCAN pilot area than in the Arucas-Moya area, although the PLOCAN area is characterized by much lower seasonal effect and unidirectional waves. The Weptos and Wave Dragon devices show less variations in percentage terms throughout the year at both sites and, thus, less variations in the percentage of demand supplied.

The results confirm that it is not possible to establish a general correlation between the wave resource and a wave farm energy output, which varies depending on the different operating principles. It is shown that the highest wave energy potential does not necessarily lead to the highest electricity production. In this respect, the appropriate choice of WEC technology is a key factor. The importance of a comprehensive analysis, starting with the farm layout, is highlighted. This situation is accentuated when the available marine region is limited, with the dimensions of the WEC devices as well as their predetermined safety distances playing a fundamental role.

In the particular case of Gran Canaria, the analysis of single devices (not in a farm configuration) found the Weptos device to be the best-adapted technology, achieving the best pairing with the wave resource and, more importantly, the highest electricity production and stability in electricity production. However, from a wave farm perspective, the surface area required for the deployment of the devices and the subsequent safety distances are critical parameters that make limits the possibilities of using this device in small areas.

From the wave farm perspective, the Wave Dragon technology appears to have a better fit in more energetic marine areas, while Wavepiston wave farms are best suited to environments with lower wave potential. However, when it comes to choosing one of these technologies for both of the pilot areas, it was observed that the decrease in Wave Dragon efficiency when it is located in a lower resource zone is higher

Appendix A. Complementary information of input database

The work data comes from “Puertos del Estado” (Spain). The SIMAR dataset consists of time series of wind and wave parameters from numerical modeling.

WaveWatch III model developed by the National Center for Environmental Prediction (NECP) of the National Oceanic and Atmospheric Administration, is a third-generation spectral model that solves the energy balance equation without establishing any a priori hypothesis about the shape of the wave spectrum [101]. This model generates hourly time-series of wave fields and use real buoys (REDCOS buoys) for final validation. All the time-series include wave characteristics like significant wave height (H_s), peak wave period (T_p) and wave direction. Fig. A.1 shows the grid of simulated data set (modelled SIMAR points in green and real REDCOS buoy points in red). The spatial resolution of the mesh has different levels, reaching ~2 km in the Canary archipelago's coasts. Fig. A.1 shows the SIMAR and REDCOS grid [63].

than the efficiency loss estimated for Wavepiston in the opposite case.

In regard to freshwater production per covered area and the percentage of electricity coverage achieved, it is confirmed that wave energy can substantially or fully satisfy desalination plant electricity demand, as long as there is a sufficient marine surface available to install the correspondingly-sized wave farm.

The inter-annual and multi-decadal analysis also confirmed that, in this particular region, there is no surge in wave energy potential that could trigger an underestimated wave farm design. However, a resource extreme value analysis could be done in future research to evaluate the farms survivability.

Another relevant conclusion is that, although the differences in terms of energy density, freshwater production per covered area and the percentage of electricity coverage for one single device are very important, they are within the same order of magnitude when it comes to wave farms in the Arucas-Moya area showing ratios of freshwater production per surface area ranging from 6.4 to 9 m³/m². The PLOCAN area shows higher variations ranging from 4.2 to 10.5 m³/m².

All in all, by selecting the appropriate WEC, wave energy would be a great alternative to desalination plants located in coastal areas.

CRediT authorship contribution statement

B. Del Río-Gamero: Conceptualization, Methodology, Investigation, Resources, Software, Data curation, Formal analysis, Writing – original draft, Validation, Writing – review & editing, Visualization. **Tyrone Lis Alecio:** Software, Data curation, Writing – review & editing. **J. Schallenberg-Rodríguez:** Conceptualization, Validation, Formal analysis, Writing – review & editing, Supervision, Project administration.

Declaration of competing interest

The authors declare the following financial interests/personal relationships which may be considered as potential competing interests: Beatriz Del Rio Gamero And Tirone Lis Alecio reports financial support was provided by European Regional Development Fund.

Acknowledgements

This research was co-funded by the ERDF and the INTERREG MAC 2014-2020 programme within the E5DES project (MAC2/1.1a/309) and the DESAL+ project (MAC/1.1a/094). No funding sources had any influence on study design, collection, analysis, or interpretation of data, manuscript preparation, or the decision to submit for publication.

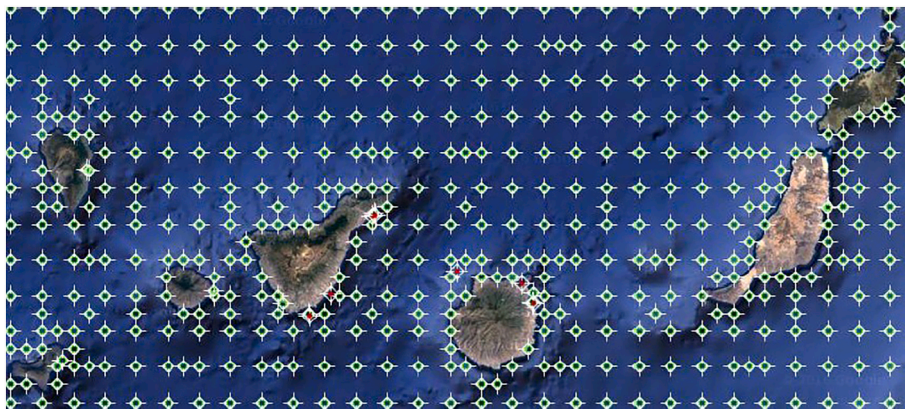


Fig. A.1. SIMAR and REDCOS grid in the Canary Island region [63].

Appendix B. Complementary information of monthly wave peak period patterns

Fig. B.1 shows a boxplot for each month of the wave peak period in Arucas-Moya pilot area. It can be seen how the highest months of wave energy potential are due to swell (defined as 10 s or more of wave peak period) originating a highly energetic wave environment. Likewise, a large variation in this parameter hinders the wave energy potential throughout the year in this area.

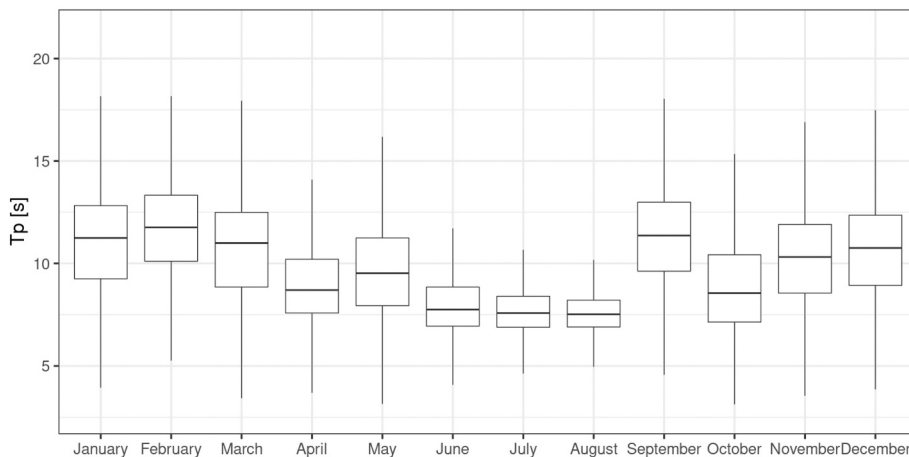


Fig. B.1. Boxplot of monthly peak wave period in the Arucas-Moya pilot area.

In contrast, Fig. B.2 shows the monthly wave peak period pattern in PLOCAN pilot area where no contribution of swell is found, but values remains much more constant thought the year.

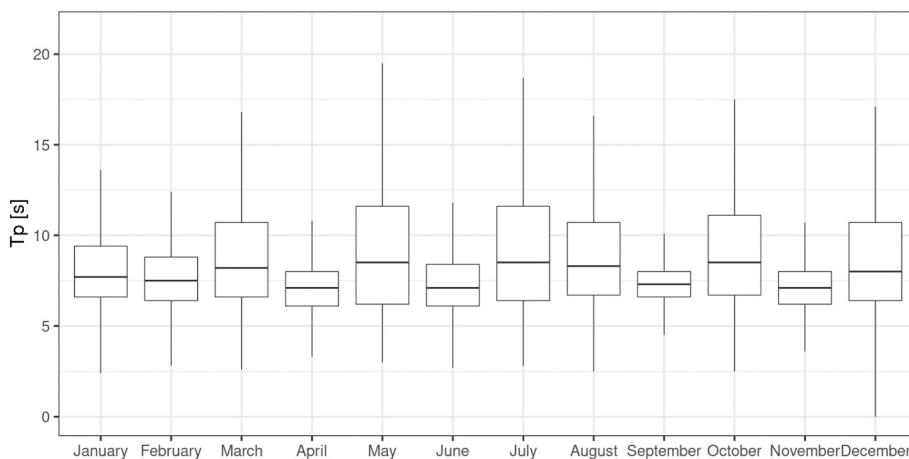


Fig. B.2. Boxplot of monthly peak wave period in the PLOCAN pilot area.

Appendix C. Inter-annual study of significant wave height and wave peak period in the Arucas-Moya and PLOCAN pilot areas

Table C1

Data values for inter-annual variation analysis.

Years	Arucas-Moya			PLOCAN		
	Mean H _s (m)	Mean T _p (s)	Max H _s (m)	Mean H _s (m)	Mean T _p (s)	Max H _s (m)
1992–1993	1.57	9.56	4.55	1.20	8.08	3.3
1993–1994	1.65	9.77	5.30	1.23	8.19	4.9
1994–1995	1.64	9.77	5.30	1.24	8.21	4.9
1995–1996	1.64	9.76	4.94	1.18	8.49	3.5
1996–1997	1.57	9.76	5.32	1.07	8.45	3.2
1997–1998	1.50	9.71	5.81	1.07	8.11	3.7
1998–1999	1.61	9.58	5.81	1.15	7.90	3.8
1999–2000	1.63	9.68	5.64	1.12	7.95	3.8
2000–2001	1.61	9.69	4.55	1.06	8.13	3.8
2001–2002	1.63	9.75	4.55	1.06	8.15	3.8
2002–2003	1.66	9.72	5.42	1.13	8.09	3.9
2003–2004	1.59	9.56	5.42	1.14	7.95	4.4
2004–2005	1.54	9.55	4.03	1.13	7.96	4.4
2005–2006	1.51	9.88	3.93	1.12	8.07	3.9
2006–2007	1.48	10.15	3.86	1.14	7.94	3.9
2007–2008	1.49	9.91	4.55	1.17	7.90	3.5
2008–2009	1.38	9.29	4.55	1.00	8.05	3
2009–2010	1.32	9.22	4.38	0.96	8.13	3.1
2010–2011	1.45	9.93	4.07	1.18	8.19	3.1
2011–2012	1.54	10.15	3.67	1.22	8.16	4
2012–2013	1.58	10.41	3.67	1.20	8.28	4
2013–2014	1.67	10.67	6.20	1.24	8.28	4.7
2014–2015	1.68	10.57	6.20	1.27	7.81	4.7
2015–2016	1.63	10.47	4.58	1.27	7.60	4.2
2016–2017	1.58	10.32	4.34	1.26	7.79	3.8
2017–2018	1.60	10.72	4.74	1.27	8.35	4.2

References

- [1] D. Fouquet, T.B. Johansson, European renewable energy policy at crossroads—focus on electricity support mechanisms, *Energy Policy* 36 (11) (2008) 4079–4092, <https://doi.org/10.1016/J.ENPOL.2008.06.023>.
- [2] M. Lange, G. Page, V. Cummins, Governance challenges of marine renewable energy developments in the U.S. – creating the enabling conditions for successful project development, *Mar. Policy* 90 (2018) 37–46, <https://doi.org/10.1016/j.marpol.2018.01.008>.
- [3] S. Salvador, L. Gimeno, F.J. Sanz Larruga, The influence of maritime spatial planning on the development of marine renewable energies in Portugal and Spain: legal challenges and opportunities, *Energy Policy* 128 (2019) 316–328, <https://doi.org/10.1016/j.enpol.2018.12.066>.
- [4] F.R. Munro, Renewable energy and transition-periphery dynamics in Scotland, *Environ. Innov. Soc. Transit.* 31 (2019) 273–281, <https://doi.org/10.1016/j.eist.2018.09.001>.
- [5] H.C. Gils, S. Simon, Carbon neutral archipelago – 100% renewable energy supply for the Canary Islands, *Appl. Energy* 188 (2017) 342–355, <https://doi.org/10.1016/j.apenergy.2016.12.023>.
- [6] H.X. Li, D.J. Edwards, M.R. Hosseini, G.P. Costin, A review on renewable energy transition in Australia: an updated depiction, Available at: *Journal of Cleaner Production* (2020) <https://doi.org/10.1016/j.jclepro.2019.118475>.
- [7] M. deCastro, S. Salvador, M. Gómez-Gesteira, X. Costoya, D. Carvalho, F.J. Sanz-Larruga, L. Europe Gimeno, China and the United States: three different approaches to the development of offshore wind energy, *Renew. Sust. Energ. Rev.* (2019) 55–70, <https://doi.org/10.1016/j.rser.2019.04.025>. Elsevier Ltd July 1.
- [8] J. Bosch, I. Staffell, A.D. Hawkes, Global levelised cost of electricity from offshore wind, *Energy* (2019), <https://doi.org/10.1016/j.energy.2019.116357>.
- [9] S. Pedersen, D. Ahsan, Emergency preparedness and response: insights from the emerging offshore wind industry, *Saf. Sci.* 121 (2020) 516–528, <https://doi.org/10.1016/j.ssci.2019.09.022>.
- [10] D.G. Caglayan, D.S. Ryberg, H. Heinrichs, J. Linßen, D. Stolten, M. Robinius, The techno-economic potential of offshore wind energy with optimized future turbine designs in Europe, *Appl. Energy* (2019) 255, <https://doi.org/10.1016/j.apenergy.2019.113794>.
- [11] C.V.C. Weiss, R. Guanache, B. Ondiviela, O.F. Castellanos, J. Juanes, Marine renewable energy potential: a global perspective for offshore wind and wave exploitation, *Energy Convers. Manag.* 177 (2018) 43–54, <https://doi.org/10.1016/j.enconman.2018.09.059>.
- [12] X. Costoya, M. deCastro, D. Carvalho, M. Gómez-Gesteira, On the suitability of offshore wind energy resource in the United States of America for the 21st century, *Appl. Energy* 2020 (262) (October 2019), 114537, <https://doi.org/10.1016/j.apenergy.2020.114537>.
- [13] J.C. Santamarta, J. Neris, J. Rodríguez-Martín, M.P. Arraiza, J.V. López, Climate change and water planning: new challenges on islands environments, *IERI Procedia* 9 (2014) 59–63, <https://doi.org/10.1016/j.ieri.2014.09.041>.
- [14] D. Curto, V. Franzitta, A. Guercio, A review of the water desalination technologies, *Appl. Sci.* 11 (2) (2021) 1–36, <https://doi.org/10.3390/app11020670>.
- [15] L. García-Rodríguez, Renewable energy applications in desalination: state of the art, *Sol. Energy* 75 (5) (2003) 381–393, <https://doi.org/10.1016/j.solener.2003.08.005>.
- [16] J.J. Sathwani, J.M. Veza, Desalination and energy consumption in Canary Islands, *Desalination* 221 (1–3) (2008) 143–150, <https://doi.org/10.1016/j.desal.2007.02.051>.
- [17] C. Charcosset, A review of membrane processes and renewable energies for desalination, *Desalination* 245 (1–3) (2009) 214–231, <https://doi.org/10.1016/j.desal.2008.06.020>.
- [18] V. Belessiotis, E. Delyannis, The history of renewable energies for water desalination, *Desalination* 128 (2) (2000) 147–159, [https://doi.org/10.1016/S0011-9164\(00\)00030-8](https://doi.org/10.1016/S0011-9164(00)00030-8).
- [19] F.E. Ahmed, R. Hashaikeh, N. Hilal, Hybrid Technologies: The Future of Energy Efficient Desalination – A Review, *Desalination* (2020), <https://doi.org/10.1016/j.desal.2020.114659>. Elsevier B.V. December 1.
- [20] M.A. Eltawil, Z. Zhengming, L. Yuan, A review of renewable energy technologies integrated with desalination systems, *Renew. Sust. Energ. Rev.* 13 (9) (2009) 2245–2262, <https://doi.org/10.1016/j.rser.2009.06.011>.
- [21] J. Leijon, D. Salar, J. Engström, M. Leijon, C. Boström, Variable renewable energy sources for powering reverse osmosis desalination, with a case study of wave powered desalination for Kilifi, Kenya, *Desalination* 494 (2020), 114669, <https://doi.org/10.1016/j.desal.2020.114669>.
- [22] N. Ghaffour, I.M. Mujtaba, Desalination using renewable energy, *Desalination* 435 (February) (2018) 1–2, <https://doi.org/10.1016/j.desal.2018.01.029>.
- [23] J. Bundschuh, M. Kaczmarczyk, N. Ghaffour, B. Tomaszewska, State-of-the-art of renewable energy sources used in water desalination: present and future prospects, *Desalination* 508 (February) (2021), <https://doi.org/10.1016/j.desal.2021.115035>.
- [24] A. Gómez-Gotor, B. Del Río-Gamero, I. Prieto Prado, A. Casañas, The history of desalination in the Canary Islands, *Desalination* 428 (2018) 86–107, <https://doi.org/10.1016/j.desal.2017.10.051>.
- [25] N. Guillou, G. Chapalain, Annual and seasonal variabilities in the performances of wave energy converters, *Energy* 165 (2018) 812–823, <https://doi.org/10.1016/j.energy.2018.10.001>.
- [26] Y. Lin, S. Dong, Z. Wang, C. Guedes Soares, Wave energy assessment in the China adjacent seas on the basis of a 20-year SWAN simulation with unstructured grids, *Renew. Energy* 136 (2019) 275–295, <https://doi.org/10.1016/j.renene.2019.01.011>.

- [27] A. Ulazia, M. Penalba, G. Ibarra-Berastegui, J. Ringwood, J. Sáenz, Reduction of the capture width of wave energy converters due to long-term seasonal wave energy trends, *Renew. Sust. Energy. Rev.* (2019) 113, <https://doi.org/10.1016/j.rser.2019.109267>.
- [28] J. Morim, N. Cartwright, M. Hemer, A. Etemad-Shahidi, D. Strauss, Inter- and intra-annual variability of potential power production from wave energy converters, *Energy* 169 (2019) 1224–1241, <https://doi.org/10.1016/j.energy.2018.12.080>.
- [29] M.V.W. Cuttler, J.E. Hansen, R.J. Lowe, Seasonal and interannual variability of the wave climate at a wave energy hotspot off the southwestern coast of Australia, *Renew. Energy* 146 (2020) 2337–2350, <https://doi.org/10.1016/j.renene.2019.08.058>.
- [30] B.C. Trewin, The role of climatological normals in a changing climate, *World Meteorol. Organ.* 1377 (2007) 6–28.
- [31] M. Penalba, A. Ulazia, J. Sáenz, J.V. Ringwood, Impact of long-term resource variations on wave energy farms: the Icelandic case, *Energy* (2020) 192, <https://doi.org/10.1016/j.energy.2019.116609>.
- [32] B.G. Reguero, I.J. Losada, F.J. Méndez, A global wave power resource and its seasonal, interannual and long-term variability, *Appl. Energy* 148 (2015) 366–380, <https://doi.org/10.1016/j.apenergy.2015.03.114>.
- [33] B. Kamranzad, A. Etemad-Shahidi, V. Chegini, Developing an optimum hotspot identifier for wave energy extracting in the northern Persian Gulf, *Renew. Energy* 114 (2017) 59–71, <https://doi.org/10.1016/j.renene.2017.03.026>.
- [34] S.P. Neill, M.R. Hashemi, Wave power variability over the northwest European shelf seas, *Appl. Energy* 106 (2013) 31–46, <https://doi.org/10.1016/j.apenergy.2013.01.026>.
- [35] M.M. Amrutha, V.S. Kumar, H. Bhaskaran, M. Naseef, Consistency of wave power at a location in the coastal waters of central eastern Arabian Sea, *Ocean Dyn.* 69 (5) (2019) 543–560, <https://doi.org/10.1007/s10236-019-01267-1>.
- [36] G. Lavidas, V. Venugopal, A 35 year high-resolution wave atlas for nearshore energy production and economics at the Aegean Sea, *Renew. Energy* 103 (2017) 401–417, <https://doi.org/10.1016/j.renene.2016.11.055>.
- [37] F. Aristodemo, D. Algieri Ferraro, Feasibility of WEC installations for domestic and public electrical supplies: a case study off the Calabrian Coast, *Renew. Energy* 121 (2018) 261–285, <https://doi.org/10.1016/j.renene.2018.01.012>.
- [38] M.A. Abdelkareem, M. El Haj Assad, E.T. Sayed, B. Soudan, Recent Progress in the use of renewable energy sources to power water desalination plants, *Desalination* 2018 (435) (November 2017) 97–113, <https://doi.org/10.1016/j.desal.2017.11.018>.
- [39] D. Clemente, P. Rosa-Santos, F. Taveira-Pinto, On the potential synergies and applications of wave energy converters: a review, *Renew. Sust. Energy. Rev.* (2021), 110162, <https://doi.org/10.1016/j.rser.2020.110162>. Elsevier Ltd January 1.
- [40] J. Leijon, C. Boström, Freshwater production from the motion of ocean waves – a review, *Desalination* (2018) 161–171, <https://doi.org/10.1016/j.desal.2017.10.049>. Elsevier B.V. June 1.
- [41] P.A. Davies, in: *Wave-powered Desalination: Resource Assessment and Review of Technology* 186, 2005, pp. 97–109, <https://doi.org/10.1016/j.desal.2005.03.093>.
- [42] D.C. Hicks, G.R. Mitcheson, C.M. Pleass, J.F. Salevan, Delboux: ocean wave-powered seawater reverse osmosis desalination systems, *Desalination* 73 (C) (1989) 81–94, [https://doi.org/10.1016/0011-9164\(89\)87006-7](https://doi.org/10.1016/0011-9164(89)87006-7).
- [43] Government of India, Statement Laid on the Table of the Rajya Sabha in Reply to (a) to (b) of Starred Question No. *310 Regarding “Technology to Harness Sea Wave Energy” to Be Answered on Monday, 2012. September 03.
- [44] A. Corsini, E. Tortora, E. Cima, Preliminary assessment of wave energy use in an off-grid minor island desalination plant, in: *Energy Procedia* 82, Elsevier Ltd, 2015, pp. 789–796, <https://doi.org/10.1016/j.egypro.2015.11.813>.
- [45] Carnegie. CETO webpage. Available at: <<https://www.carnegiece.com/project/ceto-5-perth-wave-energy-project/>> [accessed 11.22.2020].
- [46] V. Franzitta, D. Curto, D. Milone, A. Viola, in: *The Desalination Process Driven by Wave Energy: A Challenge for the Future*, 2016, pp. 1–16, <https://doi.org/10.3390/en9121032>.
- [47] A. Viola, V. Franzitta, M. Trapanese, D. Curto, in: *A Publication of IIEETA Nexus Water & Energy: A Case Study of Wave Energy Converters (WECs) to Desalination Applications in Sicily* 34, 2016, pp. 379–386, 2.
- [48] J. Schallenberg-Rodríguez, B. Del Río-Gamero, N. Melian-Martel, T. Lis Alecio, J. González Herrera, Energy supply of a large size desalination plant using wave energy. Practical case: north of Gran Canaria, *Appl. Energy* 278 (2020), 115681, <https://doi.org/10.1016/j.apenergy.2020.115681>.
- [49] M. Folley, B. Peñate, T. Whittaker, in: *An Autonomous Wave-powered Desalination System* 220, 2008, pp. 412–421, <https://doi.org/10.1016/j.desal.2007.01.044>.
- [50] D. Cheddie, A. Maharajah, A. Ramkhalawan, P. Persad, Transient modeling of wave powered reverse osmosis, *Desalination* 260 (1–3) (2010) 153–160, <https://doi.org/10.1016/j.desal.2010.04.048>.
- [51] P. Cabrera, M. Folley, Design and performance simulation comparison of a wave energy-powered and wind-powered modular desalination, *System* 514 (June) (2021), <https://doi.org/10.1016/j.desal.2021.115173>.
- [52] H. Nassrullah, S.F. Anis, R. Hashaikheh, N. Hilal, Energy for desalination: a state-of-the-art review, *Desalination* (2020), <https://doi.org/10.1016/j.desal.2020.114569>. Elsevier B.V. October 1.
- [53] P. Cabrera, J.A. Carta, J. González, G. Melián, Wind-driven SWRO desalination prototype with and without batteries: a performance simulation using machine learning models, *Desalination* 435 (2018) 77–96, <https://doi.org/10.1016/j.desal.2017.11.044>.
- [54] H.C. Gils, S. Simon, Carbon neutral archipelago – 100% renewable energy supply for the Canary Islands, *Appl. Energy* 188 (2017) 342–355, <https://doi.org/10.1016/j.apenergy.2016.12.023>.
- [55] M. Isobe, Impact of global warming on coastal structures in shallow water, *Ocean Eng.* 71 (2013) 51–57, <https://doi.org/10.1016/j.oceaneng.2012.12.032>.
- [56] C. Ozkan, K. Perez, T. Mayo, The impacts of wave energy conversion on coastal morphodynamics, *Sci. Total Environ.* 712 (2020), 136424, <https://doi.org/10.1016/j.scitotenv.2019.136424>.
- [57] K. Taniguchi, Y. Tajima, Variations in extreme wave events near a South Pacific Island under global warming: case study of tropical cyclone Tomas, *Prog. Earth Planet. Sci.* 7 (1) (2020), <https://doi.org/10.1186/s40645-020-0321-y>.
- [58] R.J. Bergillos, C. Rodríguez-Delgado, G. Iglesias, Wave farm impacts on coastal flooding under sea-level rise: a case study in southern Spain, *Sci. Total Environ.* 653 (2019) 1522–1531, <https://doi.org/10.1016/j.scitotenv.2018.10.422>.
- [59] S. Diaconu, E. Rusu, The environmental impact of a wave dragon Array operating in the Black Sea, *Sci. World J.* (2013, 2013.), <https://doi.org/10.1155/2013/498013>.
- [60] C. Rodríguez-Delgado, R.J. Bergillos, M. Ortega-Sánchez, G. Iglesias, Wave farm effects on the coast: the alongshore position, *Sci. Total Environ.* 640–641 (2018) 1176–1186, <https://doi.org/10.1016/j.scitotenv.2018.05.281>.
- [61] C. Rodríguez-Delgado, R.J. Bergillos, M. Ortega-Sánchez, G. Iglesias, Protection of gravel-dominated coasts through wave farms: layout and shoreline evolution, *Sci. Total Environ.* 636 (2018) 1541–1552, <https://doi.org/10.1016/j.scitotenv.2018.04.333>.
- [62] J. Abanades, G. Flor-Blanco, G. Flor, G. Iglesias, Dual wave farms for energy production and coastal protection, *Ocean Coast. Manag.* 160 (March) (2018) 18–29, <https://doi.org/10.1016/j.ocecoaman.2018.03.038>.
- [63] Puertos del Estado, SIMAR hindcast database. <http://www.puertos.es/es-es/occeanografia/Paginas/portus.aspx>. (Accessed 17 July 2021).
- [64] I.J. Losada, C.V. Pascual, F.J.M. Incera, R.M. Solana, S.R. Landeira, P.C. Braña, A. T. Sampedro, N.K. Burgada, Evaluación Del Potencial de La Energía de Las Olas. Estudio Técnico PER, 2011.
- [65] M. Veigas, R. Carballo, G. Iglesias, Wave and offshore wind energy on an island, *Energy Sustain. Dev.* 22 (1) (2014) 57–65, <https://doi.org/10.1016/j.esd.2013.11.004>.
- [66] M. Gonçalves, P. Martinho, C. Guedes Soares, Assessment of wave energy in the Canary Islands, *Renew. Energy* 68 (2014) 774–784, <https://doi.org/10.1016/j.renene.2014.03.017>.
- [67] M. Veigas, G. Iglesias, Wave and offshore wind potential for the Island of Tenerife, *Energy Convers. Manag.* 76 (2013) 738–745, <https://doi.org/10.1016/j.enconman.2013.08.020>.
- [68] L. Fernández Prieto, G. Rodríguez Rodríguez, J. Schallenberg Rodríguez, Wave energy to power a desalination plant in the North of Gran Canaria Island: wave resource, socioeconomic and environmental assessment, *J. Environ. Manag.* 2019 (231) (November 2017) 546–551, <https://doi.org/10.1016/j.jenvman.2018.10.071>.
- [69] R.C.R. Team, A language and environment for statistical computing. R Foundation for Statistical Computing, Vienna, Austria, Available at: <https://www.R-project.org/>, 2018. (Accessed 14 January 2021).
- [70] R program tool, ggplot2, Available at: <https://ggplot2.tidyverse.org/>. (Accessed 21 January 2021).
- [71] R program tool, geom_density, Available at: https://www.rdocumentation.org/packages/ggplot2/versions/1.0.0/topics/geom_density. (Accessed 7 February 2021).
- [72] S. Huang, S. Sheng, A. Gerthoffert, Y. Cong, T. Zhang, Z. Wang, Numerical design study of multipoint mooring systems for the floating wave energy converter in deep water with a sloping bottom, *Renew. Energy* 136 (2019) 558–571, <https://doi.org/10.1016/j.renene.2019.01.027>.
- [73] E. Friis-Madsen, Personal communication, in: *Managing Director of Wave Dragon*, 2021.
- [74] M. Henriksen, Personal communication, in: *Chief Executive Officer of Wave Piston*, 2020.
- [75] G. Verao Fernandez, P. Balitsky, V. Stratigaki, P. Troch, Coupling methodology for studying the far field effects of wave energy converter arrays over a varying bathymetry, *Energies* 11 (11) (2018) 2899, <https://doi.org/10.3390/en11112899>.
- [76] C. Beels, P. Troch, K. De Visch, G. De Backer, J. De Rouck, J.P. Kofoed, Numerical Simulation of Wake Effects in the Lee of a Farm of Wave Dragon Wave Energy Converters. Proc. 8th Eur. Wave Tidal Energy Conf. (EWTEC), Uppsala, Sweden, 2009.
- [77] T. Larsen, Personal communication, in: *Founder and CEO of Weptos A/S*, 2021.
- [78] wikipedia. Wave Dragon seen from reflector, prototype 1:4½ <https://upload.wikimedia.org/wikipedia/commons/thumb/c/ce/WaveDragon.JPG/1280px-WaveDragon.JPG?1637689190710> (accessed Nov 23, 2021).
- [79] Wavepiston. official website <https://wavepiston.dk/#our-services> (accessed Nov 23, 2021).
- [80] Weptos. Kirt x Thomsen <https://www.kirt-thomsen.com/case05> (accessed Nov 23, 2021).
- [81] J. Schallenberg-Rodríguez, N. García Montesdeoca, Spatial planning to estimate the offshore wind energy potential in coastal regions and islands. Practical case: the Canary Islands, *Energy* 143 (2018) 91–103, <https://doi.org/10.1016/j.energy.2017.10.084>.
- [82] J. Schallenberg-Rodríguez, F. Inchausti-Sintes, Socio-economic impact of a 200 MW floating wind farm in Gran Canaria, *Renew. Sust. Energy. Rev.* 148 (May) (2021), 111242, <https://doi.org/10.1016/j.rser.2021.111242>.

- [83] J. Schallenberg-Rodríguez, J. Notario-del Pino, Evaluation of on-shore wind techno-economical potential in regions and islands, *Appl. Energy* 124 (2014) 117–129, <https://doi.org/10.1016/j.apenergy.2014.02.050>.
- [84] J. Schallenberg-Rodríguez, Photovoltaic techno-economical potential on roofs in regions and islands: the case of the Canary Islands, *Methodol. Rev. Methodol. Proposal. Renew. Sustain. Energy Rev.* 20 (2013) 219–239, <https://doi.org/10.1016/j.rser.2012.11.078>.
- [85] M. Uche-Soria, C. Rodríguez-Monroy, Energy planning and its relationship to energy poverty in decision making. A first approach for the Canary Islands, *Energy Policy* 140 (March) (2020), 111423, <https://doi.org/10.1016/j.enpol.2020.111423>.
- [86] European, C. *Energy Roadmap 2050. Publications Office of the European Union*, 15.12. 2011 COM 885, 2011. Final. Brussels.; 2011.
- [87] European, C. D. G. for E. *Report of the Work of the Task Force on Mobilising Efforts to Reach the EU Energy Efficiency Targets for 2020*. Brussels, January 2019, 2019.
- [88] G. Iglesias, R. Carballo, Wave power for La Isla Bonita, *Energy* 35 (12) (2010) 5013–5021, <https://doi.org/10.1016/j.energy.2010.08.020>.
- [89] L. Margheritini, J.P. Kofoed, Weptos wave energy converters to cover the energy needs of a small island, *Energies* 12 (3) (2019), <https://doi.org/10.3390/en12030423>.
- [90] G. Iglesias, R. Carballo, Wave resource in El Hierro an island towards energy self-sufficiency, *Renew. Energy* 36 (2) (2011) 689–698, <https://doi.org/10.1016/j.renene.2010.08.021>.
- [91] Acciona Agua <https://www.acciona-agua.com/es/areas-de-ac%0Atividad/proyectos/dc-de-plantas-de-tratamiento-de-agua/idam/arucas-moya/> (accessed Jul 8, 2020).
- [92] *Oceanic Platform of the Canary Islands, Characterization of the Oceanic Coast of Arucas Moya Region*, Available at, 2020.
- [93] Plataforma Oceánica de Canarias (PLOCAN) <https://www.plocan.eu/> (accessed Oct 11, 2019).
- [94] Ó. Monterroso, M. Rodríguez, R. Riera, E. Ramos, O. Pérez, A. Sacramento, J. Z. Costa, *Cartografía Bionómica de Los Fondos Sublitorales de Jinámar (Gran Canaria)*, 2011.
- [95] A.R. Lemes, J. Luis, P. Talavera, R. Falcon, R. Arocha, J. Curbelo, L. De Lorenzo, D. Zarzo, R. Lemes, *Evolution of Production and Energy Savings in Swro Plant of Las Palmas Iii*, 2011. Elsevier B.V. October 1.
- [96] A. Muñoz Elguera, S.O. Pérez Báez, Elimination of chemical products in the pre-treatment section of Las Palmas III reverse osmosis desalination plant to control fouling, *Desalination* 437 (2018) 164–174, <https://doi.org/10.1016/j.desal.2018.02.028>.
- [97] Company, E. *Personal Communication*, 2020.
- [98] A. Pecher, J. Kofoed, *Handbook of Ocean Wave Energy*, Ocean Engi, Springer, London, 2017.
- [99] A. Pecher, J.P. Kofoed, *Handbook of Ocean Wave Energy*, 2017, <https://doi.org/10.1007/978-3-319-39889-1>.
- [100] W. Pierson, M. Lionel, A proposed spectral form for fully developed wind seas based on the similarity theory of s.a. Kitaigorodskii, *J. Geophys. Res.* 69 (1964) 5181–5190.
- [101] W. Shao, Y. Sheng, H. Li, J. Shi, Q. Ji, W. Tan, J. Zuo, Analysis of wave distribution simulated by WAVEWATCH-III model in typhoons passing Beibu Gulf, China, *Atmosphere (Basel)* 9 (7) (2018) 1–19, <https://doi.org/10.3390/atmos9070265>.